PeerJ Preprints NOT PEER-REVIEWED

Geomorphometry.org/2018

Nation-wide, general-purpose delineation of geomorphological slope units in Italy

Massimiliano Alvioli[§], Ivan Marchesini, Fausto Guzzetti
Istituto di Ricerca per la Protezione Idrogeologica
Consiglio Nazionale delle Ricerche
via Madonna Alta 126, I-06128 Perugia, Italy
[§] massimiliano.alvioli@irpi.cnr.it

Abstract—**Slope units are portions of terrain, defined by the general requirement of maximizing homogeneity within a single unit and heterogeneity between different ones. Slope units are being used to describe a variety of processes and to assess different natural hazards. An unambiguous and reproducible definition of slope units based on quantitative hydrologic and topographic criteria was previously provided by the r.slopeunits software to automatically draw slope unit polygons on a digital surface. The software contains an adaptive algorithm allowing for a flexible yet well-defined slope unit delineation, by means of an iterative procedure. It requires a digital elevation model and a few input parameters, whose values must be optimized in a sound way, by means of multiple software runs and a proper objective function. The code is designed to quickly produce results on large areas, and in this work we devised an optimization algorithm to delineate slope units over the whole Italian peninsula. We outline the rationale of the optimization procedure for a general purpose slope unit delineation within very large areas. We present preliminary results in Central Italy, specifically a slope unit mosaic in the whole area affected by the 2016 earthquake sequence. The procedure represents a well-defined framework for slope unit delineation over the whole of Italy.**

I. Introduction

Slope units are mapping units delimited by drainage and divide lines, with the further requirement that their boundaries maximize homogeneity within a single unit and heterogeneity between different ones. A proper definition of slope units (SUs) should be such that the resulting patches must be a mosaic of the study area, clustering pixels with homogeneous morphological features and separating with boundaries the differences in the same features. Existing examples of SU delineation in the literature mainly take into account either the hydrological properties of the study area, by properly selecting SU delimited by drainage and divide lines [1-3], or analyze the aspect direction of the area, and make use of clustering or segmentation algorithms [4-6]. The idea underlying the segmentation approach is very close, in principle, to our goal of defining internally homogeneous and externally distinguishable mapping units. We note, however, that segmentation results tend to be very sensitive to initial parameters, which are many and can hardly be related to the geomorphological processes under investigation. We make use of the r.slopeunits software (a GRASS GIS module, available from [7]), whose algorithm considers simultaneously hydrological properties, variability of slope aspect and size constraints, since all turn out to be equally important in defining meaningful SUs. The software performs SU delineation using a hydrological algorithm; in addition, it further constrains the boundaries and size of SUs using aspect homogeneity. The input parameter values can be optimized in an objective way by subsequent analysis of many sets of SUs for different input parameter combinations. In Ref. [7], we tested the software and optimization algorithm with an objective function taking into account simultaneously aspect segmentation quality and landslide susceptibility performance, using AUC_{ROC}, in a 2,000 km^2 area.

In this work, we aim at a general purpose SU partition on much larger areas, namely the whole Italian territory (~300,000 km^2, cf. Fig. 1). For this reason, we relax the landslide susceptibility assessment and performance measure, and retain the only aspect segmentation quality as a measure of fitness of the SU map. We present preliminary results in the area affected by the 2006 earthquake sequence in Central Italy [8,9], still substantially wider than the area considered in Ref. [7]. Moreover, we devised a new optimization algorithm since, due to the size of the area, straightforward application of the original algorithm [7] exhibits computational and conceptual limitations.

II. Methods

Partitioning an area into patches delimited by drainage and divide lines requires the definition of parameters for the underlying hydrologic model, providing a size scale of the mosaic, resulting in uneven mapping units. This is one of the major obstacles preventing a simple implementation of an automatic procedure [10-13]. As a matter of fact, the spatial extent of terrain characteristics predisposing for a geo-hydrological phenomenon (landslides, in the case of Refs. [7, 14]) is not known a priori, and

PeerJ Preprints | https://doi.org/10.7287/peerj.preprints.27066v1 | CC BY 4.0 Open Access | rec: 30 Jul 2018, publ: 30 Jul 2018

PeerJ Preprints NOT PEER-REVIEWED

it must be extracted from a DEM. In the following, we describe how the problem of the size scale can be overcome, and a specific set of SUs can be selected using sole aspect homogeneity constraints.

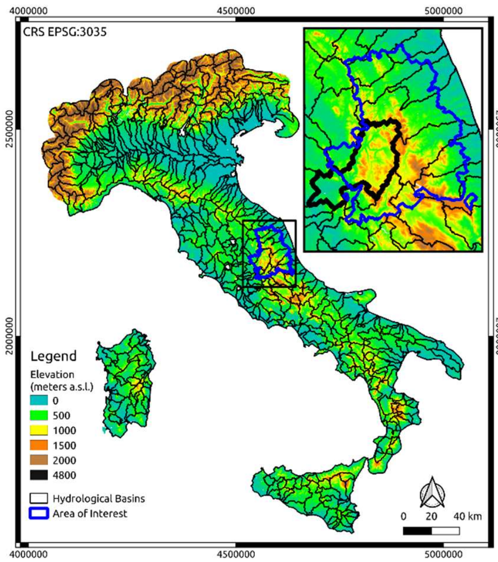

Figure 1. Subdivision of Italy in 439 hydrological basins (black polygons), within which we carried out the subsequent analyses. In this study, we selected the basins overlapping with our area of interest (blue polygon), corresponding to the municipalities affected by the 2016 earthquake in Central Italy.

A. Main algorithm

An algorithm to draw SUs is represented by the half-basins output of the module r.watershed [15] in GRASS GIS. Starting from such output, we further require that homogeneity be driven by slope aspect segmentation. Portions of half-basins with substantially different average aspect should belong to distinct SUs. We use an iterative procedure, that begins with the delineation of a half-basins set characterized by a large threshold *T*, the upslope contributing area, which is one of the input parameters. At each iteration, half-basins meeting user requirements are flagged as SUs. The remaining ones are split further at the next iteration, using a smaller value of *T*. Half-basins are promoted to SUs on the basis of two parameters: i) a planimetric area a [m^2], representing the minimum size below which a half-basin resulting from hydrologic partition corresponding to contributing area equal to *T* is considered a slope unit, and ii) a value for circular variance c of the aspect, representing the required degree of homogeneity under which a half-basin is considered an SU ($0 < c < 1$ and the smaller is its value the more the half-basin is uniform in terms of aspect) [7]. Since the upslope contributing area *T* used by the r.watershed module to extract the river network is decreased at each step of the iterative procedure, the size of the SU polygons is different in different locations of the study area, reflecting the morphological variability of the landscape. For this reason, we also define the software as adaptive. The end result is a mosaic of SU polygons whose boundaries are such that the requirements of intra-unit homogeneity and inter-unit inhomogeneity of slope aspect are fulfilled to the degree required by c, with the constraint of not crossing the hydrologic drainage and divide lines defined by *T* at each iteration. The last requirement can be partially relaxed, to a small degree, if the user requires removal of small polygons in the SU partition. Removed polygons can be merged to the adjacent ones or more complex operations can be performed, as described in detail in Ref. [7].

B. Optimization algorithm

The iterative procedure can be run for a certain number of input parameters combinations, (a, c). We suggest that the optimal combinations of input parameters can be selected, for each resulting set of SUs, by maximizing an objective function with respect to (a, c). In Ref. [7] we adapted an existing metric for the quality of image segmentation [6] to the segmentation of an aspect raster map using circular variance of the aspect, instead of aspect itself, to avoid dealing with angles. The aspect segmentation metric $F(a, c)$ is obtained from local aspect variance $V(a, c)$, and the autocorrelation index $I(a, c)$. Both are calculated with a given SU partition, hence the dependence on (a, c), as follows:

$$V = \frac{\sum_n c_n s_n}{\sum_n s_n} \tag{1}$$

and

$$I = \frac{N \sum_{n,l} \omega_{nl} (\alpha_n - \bar{\alpha})(\alpha_l - \bar{\alpha})}{\left(\sum_n (\alpha_n - \bar{\alpha})^2\right) \sum_{n,l} \omega_{nl}} \quad , \tag{2}$$

where n labels all the N SU polygons in the set delineated setting the (a, c) values of input parameters in the r.slopeunits software; c_n, s_n and α_n are the circular variance of the aspect, the surface area and the average circular variance within the n-th SU; $\bar{\alpha}$ is the average circular variance in the whole study area; ω_{nl} is an indicator for spatial proximity, equal to unity if SU polygons n and l are adjacent, zero otherwise. $V(a, c)$ represents internal aspect variance and assigns more importance to large SUs avoiding numerical instabilities produced by small ones [6], while $I(a, c)$ measures external aspect variance and has minima for SU sets exhibiting well-defined boundaries between adjacent SUs [6]. The overall function $F(a, c)$ measuring the quality of aspect segmentation is given by the normalized sum:

$$F(a,c) = \frac{V_{max} - V(a,c)}{V_{max} - V_{min}} + \frac{I_{max} - I(a,c)}{I_{max} - I_{min}} \quad . \tag{3}$$

PeerJ Preprints | https://doi.org/10.7287/peerj.preprints.27066v1 | CC BY 4.0 Open Access | rec: 30 Jul 2018, publ: 30 Jul 2018

PeerJ Preprints NOT PEER-REVIEWED

Optimization of SU delineation consists in maximizing the function in Eq. (3) as a function the (a, c) parameters. In previous works [7, 14], optimization was performed in study areas whose extent was pre-defined, i.e. determined by the extent of a landslide inventory map.

In this work, we aimed at optimization over a very large area, namely the whole Italian territory. In this case, we were faced with conceptual and computational challenges. First, the boundaries of the study area are not dictated by morphological nor process motivation, since we selected an administrative boundary. Thus, there is no reason to infer that the whole study area can be best described with a single combination of the parameters, which can be safely assumed for smaller basins. Second, the spatial extent of the study area is very large: using the EU-DEM digital elevation model, we have about 530 million valid cells, corresponding to about 330,000 km^2 (cells outside the actual Italian border were needed), at 25 m x 25 m resolution. The calculation of Eq. (2) is rather slow, due to the complex vector operations needed to find neighboring polygons, and cannot be performed on the whole study area at once with polygons of the typical SU size.

In order to make the problem computationally manageable, we devised the following solution. We prepared a subdivision of the study area in 439 hydrological basins (black polygons in Fig. 1). Each of them have size comparable with the study area of Ref. [7] (~2,000 km^2), which we maintain is a rough threshold under which optimization is not reliable. The set of basins selected for the analysis has mean area 741 km^2, with standard deviation 570 km^2; the smallest and largest basins have areas 50 km^2 and 4,300 km^2, respectively. Alluvial plains, corresponding to 117 million pixels and shown in dark green in all the Figures in this work, were removed from the SU analysis, within the r.slopeunits software.

The actual optimization of the software input parameters was performed separately in domains of increasing size, keeping the basins shown in Fig. 1 as the basic analysis elements in the following way. To obtain optimal (a, c) in the j-th basins, we first maximized F(a, c) in the basin itself. Next, we searched the maximum within the area constituted by basins j and k, where k is any of the basins adjacent to j. Next, we considered all the possible triplets of adjacent basins including j, and so on up to groups of N neighboring basins; we used N = 5 at best. We computed a weighted average of the resulting parameters as follows:

$$c_{opt}^{(N,j)} = \frac{\sum_{n=1}^{N}(N-n+1)\bar{c}_j^{(n)}}{\sum_{n=1}^{N} n} \quad , \qquad (4)$$

where

$$\bar{c}_j^{(n)} = \frac{\sum_{i=1}^{n} c_i\, s_i}{\sum_{i=1}^{n} s_i} \qquad (5)$$

and c_i is the optimal c found in the i-th combination of n basins and s_i is the corresponding total surface area. Following this procedure, for the j-th basin, j=1,..,439, we have a sequence $(c_{opt}^{(1,j)}, c_{opt}^{(2,j)}, \dots, c_{opt}^{(5,j)})$ of values. If the sequence admits an asymptote, we used this value as the optimal one, otherwise we used the local maximum as our optimal value. The procedure was applied both for circular variance, c, and minimum area, a.

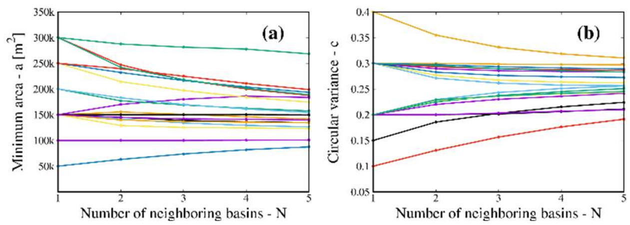

Figure 2. The values of the optimal parameters a (a) and c (b) as a function of the number of neighboring basins, N, used in Eq. (4). The curves correspond to a subset (18 out of 439) of the basins denoted with black polygons in Fig. 1.

III. Results and Conclusions

We present results for the subset of basins overlapping with the study area, the blue polygon in Fig. 1. For the purpose, we performed the parameter optimization for the basins overlapping the mentioned area, namely the black polygons in Fig. 1.

Figure 2 shows the values of $(c_{opt}^{(1,j)}, c_{opt}^{(2,j)}, \dots, c_{opt}^{(5,j)})$ and $(a_{opt}^{(1,j)}, a_{opt}^{(2,j)}, \dots, a_{opt}^{(5,j)})$ for the considered basins, demonstrating the tendency of both series to converge to an asymptote. This was expected, due to the definition in Eq. (4) containing smaller weights for $\bar{c}_j^{(n)}$ with increasing n, but convergence is still not obvious and it actually does not hold for all of the considered basins.

Figure 3 shows the objective function F(a, c) for one of the considered basins, namely the one highlighted with a thick black line in the inset of Fig. 1. The purple surface was obtained on a pre-defined grid of values for (a, c) pairs, while the blue curve was obtained with a maximum-bracketing algorithm developed for the purpose which will be published with the upcoming version of r.slopeunits. Purple and blue bullets represent maxima in the two cases. The former occurs at $(a_{opt}^{(1)}, c_{opt}^{(1)})$ for the basin under investigation, and the latter represents the fallback values of our algorithm, adopted when the procedure leads to no asymptotic convergence.

Figure 4 shows the optimal set of SUs obtained for a sample basin among those considered in Fig. 1; we do not show SU maps for the other basins due to lack of space. The SU delineation for

PeerJ Preprints | https://doi.org/10.7287/peerj.preprints.27066v1 | CC BY 4.0 Open Access | rec: 30 Jul 2018, publ: 30 Jul 2018

all the basins overlapping with the area of interest shown in Fig. 1 is available in vector format.

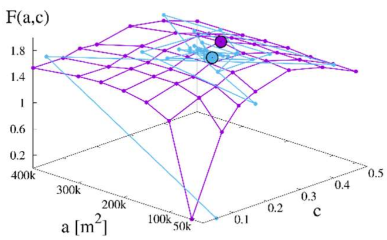

Figure 3. The aspect segmentation metric $F(a, c)$ of Eq. (3), calculated in the basin shown with a thick black line in Fig. 1. The purple curve shows $F(a, c)$ calculated on a predefined grid, while the blue curve was obtained by an automatic search algorithm. The two maxima, denoted by bigger circles, may not appear at the same vertical height since there is a dependence on the minimum and maximum values of $F(a, c)$ within the same optimization run.

In conclusion, we devised a robust and reproducible process for SU delineation over large areas, based on the parametric software r.slopeunits [7]. We tested the procedure in a large area in Central Italy, shown in Fig 1. A sample of the results is shown in Fig. 4 for a single basin, for illustration purposes. Since we optimized the delineation by maximizing the quality of aspect segmentation, we expect the resulting SUs to be suited for all the geo-environmental applications that require identification of domains facing distinct directions. These may be represented by, but are not limited to, studies involving different natural hazards, or a combination of them, as well as hydrological studies, agricultural applications, land use studies, and others [16].

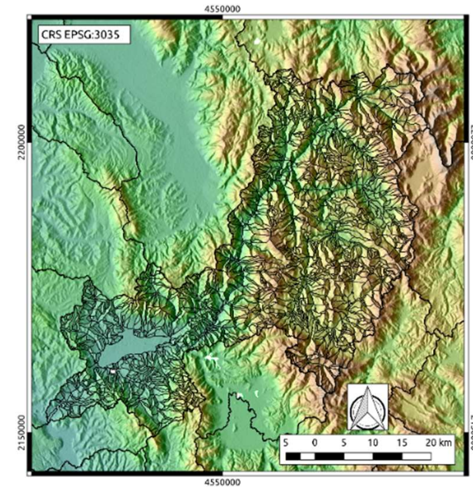

Figure 4. The final slope unit subdivision (black polygons) obtained as a result of the optimization procedure described in this work, in the basin shown with a thick black line in Fig. 1, overlapping with the area of interest.

REFERENCES

[1] Carrara, A., M. Cardinali, R. Detti, F. Guzzetti, V. Pasqui, P. Reichenbach, 1991. "GIS Techniques and statistical models in evaluating landslide hazard. Earth Surf. Process. Landform 16, 427–445.

[2] Carrara, A., 1998. "Drainage and divide networks derived from high-fidelity digital terrain models". Vol. 223 of Quantitative Analysis of Mineral and Energy Resources - Mathematical and Physical Sciences, D. Reidel Publishing Company, pp. 581-597.

[3] Guzzetti, F., M. Cardinali, P. Reichenbach, A. Carrara, 2000. "Comparing Landslide Maps: A Case Study in the Upper Tiber River Basin, Central Italy". Environ. Manage. 25, 247-263.

[4] Flanders, D., M. Hall-Beyer, J. Pereverzoff, 2003. "Preliminary evaluation of eCognition object-oriented software for cut block delineation and feature extraction". Can. J. Remote Sens. 29, 441-452.

[5] Drăgut, L., O. Csillik, C. Eisank, D. Tiede, 2014. "Automated parameterisation for multi-scale image segmentation on multiple layers". ISPRS J. Photogramm. Remote Sens. 88, 119-127.

[6] Espindola, G.M., G. Camara, I.A. Reis, L.S. Bins, A.M. Monteiro, 2006. "Parameter selection for region-growing image segmentation algorithms using spatial autocorrelation". Int. J. Remote Sens. 14, 3035-3040.

[7] Alvioli, M., I. Marchesini, F. Fiorucci, F. Ardizzone, M. Rossi, P. Reichenbach, F. Guzzetti, 2016. "Automatic delineation of geomorphological slope units with r.slopeunits v1.0 and their optimization for landslide susceptibility modeling". Geosci. Model Dev., 9, 3975–3991, 2016.

[8] Galli, P., B. Giaccio, P. Messina, E. Peronace, 2016. "Three magnitude 7 earthquakes on a single fault in central Italy in 1400 years, evidenced by new palaeoseismic results". Terra Nova 28(2), 146–154.

[9] Guzzetti, F., M. Cardinali, P. Reichenbach, 1996. The influence of structural setting and lithology on landslide type and pattern. Environmental and Engineering Geoscience 2, 531-555.

[10] Erener, A. and S.B. Düzgün, 2012. "Landslide susceptibility assessment: what are the effects of mapping unis and mapping method?". Environ. Earth Sci. 66, 859-877.

[11] Zhao, M., F. Li, G. Tang, 2013. "Optimal Scale Selection for DEM Based Slope Segmentation in the Loess Plateau". Int. J. Geosci. 3, 37-43.

[12] Sharma, R.K. and B.S. Mehta, 2012. "Macro-zonation of landslide susceptibility in Garamaura-Swarghat-Gambhar section of national highway 21, Bilaspur District, Himachal Pradesh (India)". Nat. Hazards 60, 671-688.

[13] Mashimbye, Z.E., W.P. de Clerq, A. Van Niekerk, 2014. "An evaluation of digital elevation models (DEMs) for delineating land components". Geoderma 231, 312-319.

[14] Schlögel, R., I. Marchesini, M. Alvioli, P. Reichenbach, M. Rossi, J.-P. Malet, 2018. "Optimizing landslide susceptibility zonation: Effects of DEM spatial resolution and slope unit delineation on logistic regression models". Geomorphology, 301, 10-20.

[15] Metz, M., H. Mitasova, R. S. Harmon, (2010). "Efficient extraction of drainage networks from massive, radar/based elevation models with least cost path search". Hydrology and Earth System Sciences 15, 667-678.

[16] Alvioli, M., A. C. Mondini, F. Fiorucci, M. Cardinali, I. Marchesini, 2018. "Topography-driven satellite imagery analysis for landslide mapping". Geomatics, Natural Hazards & Risk. 9(1), 544-567.

PeerJ Preprints | https://doi.org/10.7287/peerj.preprints.27066v1 | CC BY 4.0 Open Access | rec: 30 Jul 2018, publ: 30 Jul 2018